RC 21891 (98484) 9 November 2000 **Electrical Engineering**

IBM Research Report

Strength of Electric Field in Apertureless Near-Field Optical Microscopy

Yves C. Martin, Hendrick F Hamann , Kumar Wickramasinghe
IBM Research Division
Thomas J. Watson Research Center
P. O. Box 218
Yorktown Heights, NY 10598

Research Division
Almaden - Austin - Beijing - Haifa - T. J. Watson - Tokyo - Zurich

Strength of electric field in apertureless near-field optical microscopy

Yves C. Martin, Hendrik F. Hamann and H. Kumar Wickramasinghe*

IBM, T.J.Watson Research Center

P.O.Box 218

Yorktown Heights, NY 10598

ABSTRACT

Enhancement γ of the electrical field at the end of a tip relative to the incident field in a focused radiation beam is calculated by a Finite Difference Time Domain (FDTD) method. First, the reliability of the FTDT method is established by calculating the electric field on simple structures like thin cylinders, spheres and ellipsoids, and comparing the results with analytical solutions. The calculations on these test structures also reveal that phase retardation effects substantially modify γ when the size of the structure is larger than approximately $\lambda/4$, λ being the radiation wavelength. For plasmon resonance in particular, phase retardation severely reduces the resonance and the expected field enhancement for a gold tip. The small value of $\gamma = 4$ calculated by FDTD is about an order of magnitude smaller than the value found in recent published work.

Resonance effects can be recovered for special tips, which have a discontinuity or a different material composition at the end of the tip. Some tuning of the discontinuity dimension is needed to maximize the resonance. Under optimal conditions for plasmon resonance, an enhancement in electric field of about 50 is calculated at the end of a small gold protrusion mounted on a wider silicon or glass tip.

* for correspondence

1. Introduction

Field enhancement at the end of a sharp tip has been studied and utilized in optical harmonic generation and optical rectification in cat's whisker diodes since the early experiments of Javan et al., several decades ago [1-4]. In apertureless near-field scanning optical microscopy (NSOM) [5], the localized optical interaction between a probe tip and sample is exploited for high resolution imaging and spectroscopy on a nanometer scale. The technique has been successfully demonstrated for coherent[6-14], fluorescence [15] and non-linear [16-18] imaging. In order to maximize the optical near-field interaction, a strong field $|E_{NF}|$ at the end of the probe is desirable, which is typically generated by the optical field $|E_o|$ of a focused laser. It has been pointed out by many authors [19-23] that it is important to have a component of $|E_o|$ pointing along the tip axis in order to enhance the field $|E_{NF}|$ at the end of the tip as in the experiments with cat's whisker diodes. Indeed, in our early demonstrations of apertureless near-field microscopy the tips were tilted over a range from 45° [6,9] to 10° [10, 24] relative to the incident beam axis, to provide some field enhancement as well as rejection of specularly reflected light.

Achieving a substantial optical near-field enhancement $\gamma = |E_{NF}|/|E_o|$ at the end of a nanoscopic probe is a key challenge for a number of novel applications ranging from data storage[24], surface modification [25], multi-photon molecular fluorescence spectroscopy [16-18] to optical tweezing at nanoscale resolution [19]. The importance of a strong enhancement in combination with the idea of apertureless NSOM has stimulated recent experimental and theoretical studies [26-31]. Several recent theoretical studies have predicted large field enhancement, $\gamma = 10$ to 100, particularly when plasmon resonance is considered and when the tip is modeled as a finite ellipsoid solid. In this paper we will show computer modeling work which seems to contradict some of these results. Modeling the tip as a semi-infinite solid seems to diminish the predicted enhancement numbers significantly, which we attribute to phase retardation or dephasing effects.

The work described here is based on finite difference time domain modeling (FDTD)[23,32], which takes into account all electromagnetic interactions on the scale of a few wavelengths in three dimensions. In the first part, we review the different pieces of the underlying physics of the electric field enhancement, namely antenna and plasmon resonance with particular emphasis on phase retardation contributions. Furthermore, by illustrating these different phenomena using simple structures (such as thin wires, spheres and ellipsoids) we prove the

reliability and accuracy of our calculations by comparing it with known and rigorous solutions. In the second part, we discuss the electric field enhancement of real tip systems. Surprisingly, we find significantly lower field enhancement than previous studies. We attribute this to a strong contribution from dephasing effects. Finally, we demonstrate that these limitations can be overcome in specific cases by creating a tip with a discontinuity, such as a plasmon resonating ellipsoid at the end of a non-resonant tip.

2. Electric field enhancement: the role of dephasing effects

The purpose of this section is twofold. First, we review some aspects of the underlying physics for electric field enhancement and point out the importance of antenna resonance and phase retardation effects. Second, by solving electric fields for structures where analytical solutions are known, we assess the accuracy of the FDTD software [32].

Antenna resonance of thin wires:

First, we review briefly simple resonant enhancement effects of a thin perfectly conducting wire, which we model with a high dielectric constant ($\varepsilon = 10^5 + 10^5 i$). Fig.1 shows the FDTD calculations of the electric field enhancement (γ) at the end of such a wire as a function of its length a , with a constant width of 20 nm . The illumination source is a plane wave with linear polarization parallel to the wire. In agreement with antenna theory [33], we find maxima for the field when the length of the wire approximately equals an odd integer multiple of half a wavelength ($a = n\lambda + \lambda/2$, with n = 1, 2, ...). Furthermore, when the wire is not perfectly thin, the theory predicts that the peaks are shifted to the left and that the higher order peaks are lower [33]. Both these effects are also illustrated by FDTD calculations. Adjusting the length is similar to tuning an LC circuit into resonance. An increased electric field at the both ends is found when the length of the antenna matches the phase of the propagating wave. Fig.1 demonstrates that the adjustment of antenna length is critical, and that dephasing effects can reduce the enhancement by an order of magnitude. We also observe that a very long antenna produces an enhancement substantially lower than a properly tuned short antenna.

Antenna resonance of ellipsoids:

Second, we investigate how resonance or phase matching effects influence the enhancement of an elongated ellipsoidal structure (e.g. a "fat" antenna). Fig.2 shows the near-field enhancement at the end of a perfectly

conducting ellipsoid ($\varepsilon = 10^5 + 10^5 i$), calculated by FDTD, as a function of the length a of the ellipsoid. The driving field is polarized parallel to the long axis of the ellipsoid, and the ratio of long to short axis, a/b, is kept constant and equal to 3. Comparing Fig.2 to Fig.1, we find that the antenna resonance of the ellipsoid is shifted to lower lengths a ; e.g. dephasing effects modify the enhancement even at smaller sizes. Most interestingly, the higher order resonance peaks are greatly diminished demonstrating that resonance enhancements contribute positively for short ellipsoids only, and that dephasing effects reduce the enhancement for larger ones.

The ellipsoidal structure allows us to compare our result in the limit of a small length a with an analytical solution. For an elongated ellipsoid with dimensions small compared to the wavelength λ, the field enhancement factor (γ) has a simple expression [21]:

$$\gamma = \left| \frac{\varepsilon}{1+(\varepsilon-1)\cdot A} \right| \qquad (1)$$

where ε is the complex dielectric constant and A is the depolarization factor which depends on the axis ratio r = a/b of the ellipsoid,

$$A := \frac{1}{2\cdot r^2} \cdot \int_0^{\infty} \frac{1}{(s+1)^{\frac{3}{2}} \cdot \left(s + r^{-2}\right)} ds \qquad (2)$$

In this quasi-static regime, the enhancement results from the geometrical crowding of the electric lines at the narrow ends of the tip. For a thin and long conductor, r is very large and the resulting enhancement, $\gamma = |\varepsilon|$, can be very large too. This describes the lightning rod effect. For our ellipsoid, A = 0.109 and γ = 9.2. The value found by FDTD is somewhat smaller [34], but agrees within 20% with this value, which again shows the validity of FDTD results.

In order to demonstrate these effects for real metal systems, the field enhancement γ has been calculated for a tungsten ellipsoid (ε = 4.78 + 21.181 i at λ = 633nm, a/b=3). As seen in Fig.2, the resonance peak is lower and γ is also drastically reduced at large length a. From both plots in Fig.2, it can be concluded that dephasing effects decrease γ substantially when the ellipsoid becomes larger than about $\lambda/2$.

Plasmon resonance of spheres:

Third, we investigate how dephasing effects modify another type of resonance which originates from plasmons. For a limited number of metals, principally silver and gold in the visible wavelength range, plasmon resonance can become a major factor for field enhancement. Different from antenna (or geometric) effects, plasmons result from long-range correlation of electrons caused by Coulomb forces [35]. For a small ellipsoid or sphere in the quasistatic limit, plasmon resonance occurs when the real part of the denominator of Eq.(1) becomes zero, $\mathrm{Re}\{1+(\varepsilon-1)\times A\}= 0$. In the case of a sphere ($A = 1/3$), the resonance is met when the real part of the dielectric constant becomes -2. The imaginary part determines the magnitude of the resonance. For silver, the resonance occurs at $\lambda = 354$ nm, where $\varepsilon = -2 + 0.602$ i. The enhancement is $\gamma = 10.5$. Fig.3 shows γ outside the sphere and along the direction of the incident field as a function of the diameter of the sphere. The solid line is derived from a full MIE analytical calculation [36] which describes the scattering of a sphere with arbitrary size. Good agreement between MIE and FDTD results is obtained over the whole range of values. These results also show that phase retardation modifies plasmon resonance even severely even than they modify antenna resonance. Here, γ decreases by more than 3.5 at higher order peaks. In addition, we note that the first plasmon resonance peak occurs only at a very small sphere size, and that it vanishes when the sphere radius is larger than $\lambda/10$.

Plasmon resonance of ellipsoids:

Fourth, we demonstrate that phase retardation severely diminishes plasmon resonance in elongated ellipsoids. According to Eq.(1), for a small ellipsoid with $a/b = 3.5$, plasmon resonance is found when $\varepsilon_r = -10$. For gold, this occurs near $\lambda = 633$ nm. Fig.4 shows the field enhancement γ at the end of the ellipsoid as a function of a and for two constant aspect ratios, $r = 3.2$ and $r = 3.0$. For small sizes, γ is very large and depends strongly on the exact aspect ratio. The analytical values are 55 and 36 for aspect ratios of 3.2 and 3.0, respectively. The FDTD calculations yield 75 and 50 respectively. This is reasonable, considering that the ellipsoids are represented by finite rectangular elements [37].

In agreement with the results above, the following general conclusions can be drawn from Fig.4. First, it is demonstrated that FDTD indeed matches analytical solutions fairly well confirming our confidence in the calculation. Second, drastic dephasing effects occur when the ellipsoid is larger than $\lambda/10$. In some cases, dephasing shifts the plasmon resonance to produce a small peak; on Fig. 4, this can be observed at $a = 0.15\,\lambda$ for $r = 3.0$. However in all cases, when the ellipsoid is larger than $\lambda/2$, plasmon resonance becomes ineffective

and γ is small. Finally, a substantial near-field enhancement ($\approx$50) can be obtained if dephasing effects are circumvented.

4. Electric field enhancement for real tip systems

Having demonstrated the severe influence of dephasing effects on the field enhancement it is important to realize that real tips resemble more a semi-infinite solid (a semi-infinite cone) than a finite scatterer (cylinder or ellipsoid). Therefore, resonance conditions are substantially different than found previously, both for antenna and plasmon resonance. Fig.5 shows the calculated field at the end of silicon and gold tips. The tips are modeled as 5 degree cones terminated by hemispheres of radius R = 10nm. The illumination is a focused Gaussian beam aimed at the tip end polarized parallel to the tip (1/e beam waist radius ω_o = 0.35 μm, wavelength λ = 633nm). Fig.5 plots the enhanced vertical field at the end of the tips, revealing that field enhancement is localized to an area with dimension of the tip radius.

Calculations have been made for several materials with the same conditions. The field enhancement factors γ are given in Table I. These values are similar to previously reported values, except for gold. The value of 4 found by FDTD is significantly smaller [38] than values reported before [19-22]. Our finding seems to agree with the observations above, that dephasing effects strongly reduce plasmon resonance when the scatterer is large in comparison to the wavelength. One might think that the antenna resonance condition for a small scatterer in a plane wave can also be met for a large scatterer in a tightly focused beam. However, we find that this is not the case. Changing the beam waist radius from 1μm down to 0.22 μm modifies γ by less than a factor 2.

5. Modified tips

One possibility for recovering some resonance and thus some electric field enhancement is to create a discontinuity in the dimension of the tip. Fig.6 shows an example for Aluminum. In this example, a small protrusion extends from a larger stub. If the stub acts as a perfect reflector and the protrusion is a thin and good conductor, resonance is met when the length of the protrusion is $\lambda/4$. Because these conditions are not perfectly met for aluminum, maximum γ is found at a protrusion length of 65 nm, or 0.1λ, and γ = 11.

For gold where plasmon resonance is available, a discontinuity is generated by placing a portion of a gold ellipsoid at the end of a wider tip which can be made out of a different material [39]. Fig.7 shows the calculated field distribution for a semi-ellipsoid mounted on a wide silicon tip. A large enhancement γ = 46

can be obtained by optimizing the aspect ratio(r=3.2) and length (a/2=0.075λ) of the semi-ellipsoid. In this configuration, the enhancement depends critically on the shape and size of the gold protrusion and on the material below it. For example, changing the aspect ratio of the ellipsoid down to r = 3.0 reduces the enhancement to $\gamma = 39$. Replacing the tip material to aluminium reduces the maximum γ to about 30, but a glass tip with ¾ of a gold ellipsoid raises γ to about 50.

A wide-angle tip can also improve γ. In a last series of calculations, we modeled the tip as a wide 90-degree cone [17] terminated by a hemisphere of radius R = 10nm, and considered the same illuminating conditions and material types as before in Table I. The calculated field enhancement results are given in Table II. The largest difference between Table II and Table I is obtained for gold, where an enhancement of 14 is calculated for a wide tip, instead of 4 for the narrow tip. Dephasing effects may be less pronounced in a wide-cone tip than in a narrow-cone tip. Although the enhancement is not as high as with the previous example of a gold protrusion on a silicon tip, a solid wide-angle gold tip may be easier to produce in a reliable way.

6. Conclusion

Enhancement of the electrical field at the end of a scattering tip is substantially different from what could be estimated from simple analytical solutions for a small scatterer, when some resonance is involved. We attribute the difference to phase retardation effects that modify the resonance condition. For plasmon resonance in particular, phase retardation severely reduces the resonance and the expected field enhancement for a gold tip. The small value of about 4 that we find by FDTD calculations appear to contradict recent published work. Good confidence in the FDTD calculation is gained from tests on different types of models where agreement with analytical solutions is found: antenna-like resonator showing resonance at odd integer multiples of half a wavelength, plasmon resonance effects on a silver sphere as a function of the sphere radius, and enhancement for small ellipsoids with or without plasmon resonance.

Resonance effects can be recovered for special tips, having some discontinuity or different material composition at the end of the tip. Some tuning of the discontinuity dimension is needed to maximize the resonance. Under optimal conditions for plasmon resonance, we showed that an enhancement in E field of about 50 can be produced at the end of a small gold protrusion mounted on a wider silicon or glass tip.

Acknowledgement: The authors would like to thank Lukas Novotny for insightful exchange of correspondance, and comparison of results.

References

1. L.O.Hocker, D.R.Sokoloff, V.Daneu, A.Szoke, and A.Javan, Appl.Phys.Lett. **12**, 401(1968)

2. K.M.Evenson, J.S.Wells, L.M.Matarrese, and L.B.Elwell, Appl.Phys.Lett. **16**, 159(1970)

3. H.Q.Nguyen, P.H.Cutler, T.E.Feuchtwang, Z.Huang, Y.Kuk, P.J.Silverman, A.A.Lucas, and T.E.Sullivan, IEEE Trans.on Electron Devices **36**, 2671(1989)

4. Th.Gutjahr-Loser, A.Hornsteiner, W.Krieger, and H.Walther, J. Appl.Phys. **85**, 6331(1999)

5. H.K.Wickramasinghe and C.C.Williams, Apertureless Near Field Optical Microscope, U.S.Patent 4,947,034 (April 28, 1989)

6. F.Zenhausern, M.P.O'Boyle, and H.K.Wickramasinghe, Appl.Phys.Lett. **65**, 1623 (1994)

7. R.Bachelot, P.Gleyzes, and A.C. Boccara, Microscop. Microanal. Microstruct. **5**, 389 (1994)

8. Y. Inouye and S. Kawata, Optics Lett. **19**, 159 (1994)

9. F.Zenhausern, Y.Martin, and H.K.Wickramasinghe, Science **269**, 1083 (1995)

10. Y.Martin, F.Zenhausern, and H.K.Wickramasinghe, Appl.Phys.Lett. **68**, 2475 (1996)

11. C.Hubert and J.Levy, Appl.Phys.Let. **73**, 3229(1998)

12. S.Gresillon, H.Cory, J.C.Rivoal, and A.C.Boccara, J.Opt.A: Pure Appl.Opt. **1**, 178(1999)

13. B.Knoll and F.Keilmann, Nature **399**, 134(1999)

14. C.J.Hill, P.M.Bridger, G.S.Picus, and T.C.Mc Gill, Appl. Phys. Lett. **75**, 4022 (1999)

15. H.F.Hamann, A.Gallagher, and D.J.Nesbitt, Appl.Phys.Lett. **76**, 1953 (2000)

16. J.Wessel, J.Opt.Soc.Am.B **2**, 1538 (1985)

17. Yoshimasa Kawata, Chris Xu, and Winfried Denk, J.Appl.Phys. **85**, 1294 (1999)

18. E.J.Sanchez, L.Novotny, and X.S.Xie, Phys.Rev.Lett. **82**, 4014(1999)

19. L.Novotny, R.X.Bian, and X.S.Xie, Phys.Rev.Lett. **79**, 645 (1997)

20. L.Novotny, E.J.Sanchez, and X.S.Xie, Ultramicroscopy **71**, 21 (1998)

21. J.Jersch, F.Demming, L.J.Hildenhagen, and K.Dickmann, Appl.Phys.A **66**, 29 (1998)

22. F.Demming, J.Jersch, K.Dickmann, and P.I.Geshev , Appl.Phys.B **66**, 593 (1998)

23. H.Furukawa and S.Kawata, Optics Communications **148**, 221 (1998)

24. Y.Martin, S.Rishton, and H.K.Wickramasinghe, Appl.Phys.Lett. **71**, 1(1997)

25. J.Jersch, F.Demming, and K.Dickmann, Appl.Phys.A **64**, 29(1997)

26. Olivier J.F.Martin and Christian Girard, Appl.Phys.Lett. **70**, 705(1997)

27. I.Sh.Averbukh, B.M.Chernobrod, O.A.Sedletsky, and Y.Prior, Opt.Comm. **174**, 33(2000)

28. H.Cory, A.C.Boccara, J.C.Rivoal, and A.Lahrech, Microwave and Opt.Technology Let. **18**, 120(1998)

29. I A.V.Zayatas, Opt.Comm. **161**, 156 (1999)

30. P.M.Adam, P.Royer, R.Laddada, and J.L.Bijeon, Appl.Opt. **37**, 1814(1998)

31. M.Ashino and M.Ohtsu, Appl.Phys.Lett. **72**, 1299(1998)

32. EMFLEX by Weidlinger Associates Inc., Los Altos, CA

33. W.L.Stutzman, G.A.Thiele, *Antenna theory and design* (J.Wiley & Sons, 1981), see p.199, 200 and 202

34. One reason for this limited accuracy is the finite size of the rectangular elements that represent the ellipsoid, particularly when the ellipsoid is very small. The effective aspect ratio, r, of the finite element model may be smaller than the expected ratio r = 3, which then yields a smaller enhancement γ.

35. C.F.Bohren, D.R.Huffman, *Absorption and Scattering of Light by Small Particles* (J.Wiley & Sons, 1983)

36. J.Stratton, *Electromagnetic Theory* (McGraw-Hill New York, 1951), p.564

37. For small ellipsoid dimensions, the number of rectangular elements that map the ellipsoid is limited. The effective aspect ratio can vary by +/- 5%. Since the plasmon resonance is so strongly dependent on the aspect ratio according to equation (1), the difference found between FDTD and the analytical value is acceptable.

38. We have also repeated the exact conditions as found in [19] and [20] and found a significantly lower field enhancement γ -about 10x

39. Squalli, M.-P.Bernal, P.Hoffmann, and F.Marquis-Weible, Appl.Phys.Lett. **76**, 2134 (2000)

Table I: Field enhancement factor γ calculated by FDTD for tips made out of different material. The tip is modeled as a 5 degree angle cone terminated by a 10nm radius hemisphere. γ is given at a point approximately 2 nm below the tip.

	Silicon	Tungsten	Aluminum	Gold
ε	15	4.78 + 21.181 i	-56 + 20.7 i	-10.842 + 0.762 i
γ	6	4.9	7.4	4

Table II: Field enhancement factor γ at the end of wide tips. Tips are modeled as 90 degree (full angle) cones terminated by 10nm radius hemispheres. Other conditions are similar to those in Table I.

	Silicon	Tungsten	Aluminum	Gold
γ	4.7	5.8	9.5	14

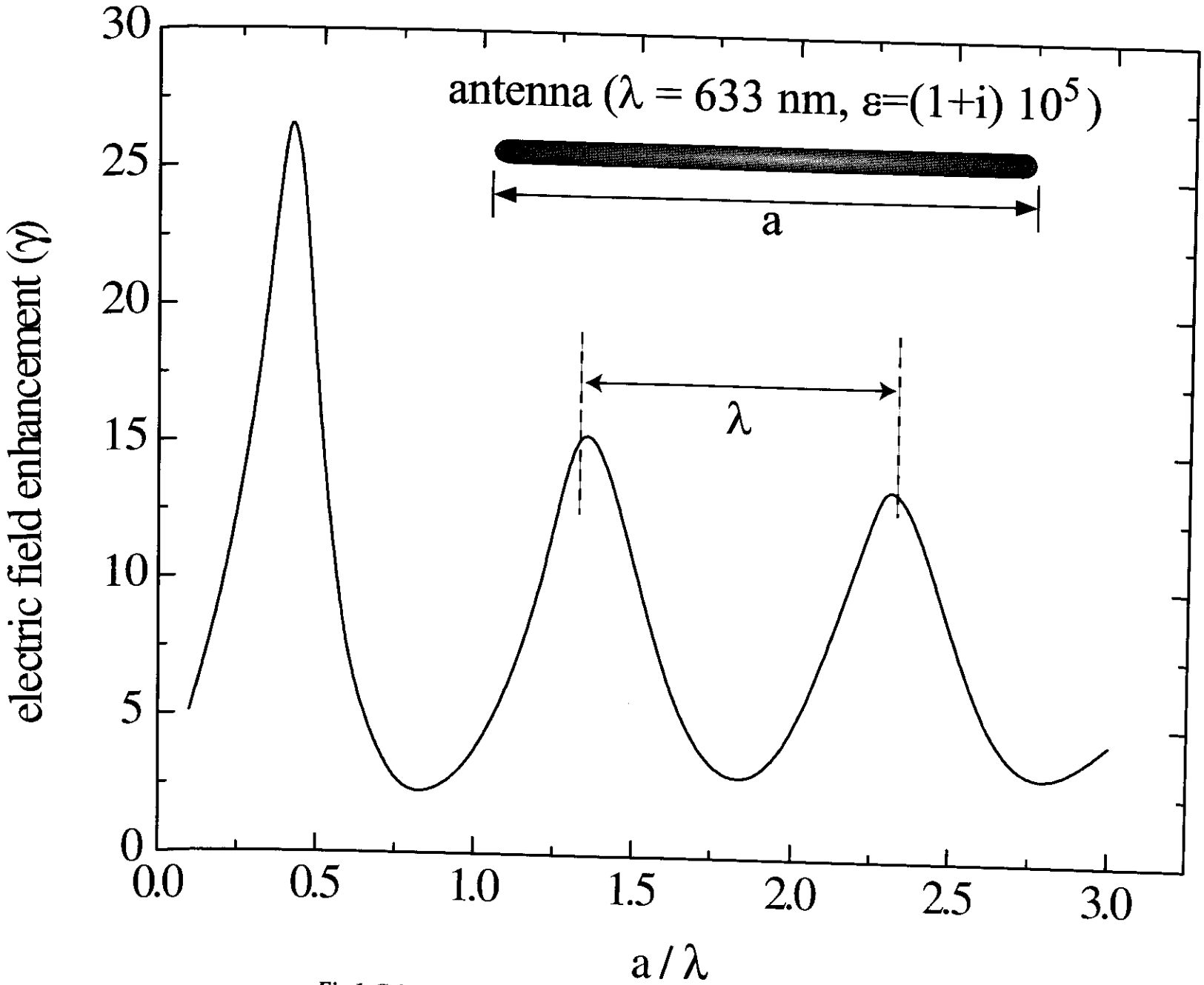

Fig.1 Calculated field enhancement γ at the end of a thin and good conductor in a plane wave. The conductor is modeled as a cylinder with a diameter of 20nm, terminated by two hemispheres. Wavelength is $\lambda = 633$ nm. Peaks due to antenna resonance appear as expected , slightly lower than odd integer multiples of half a wavelength [33].

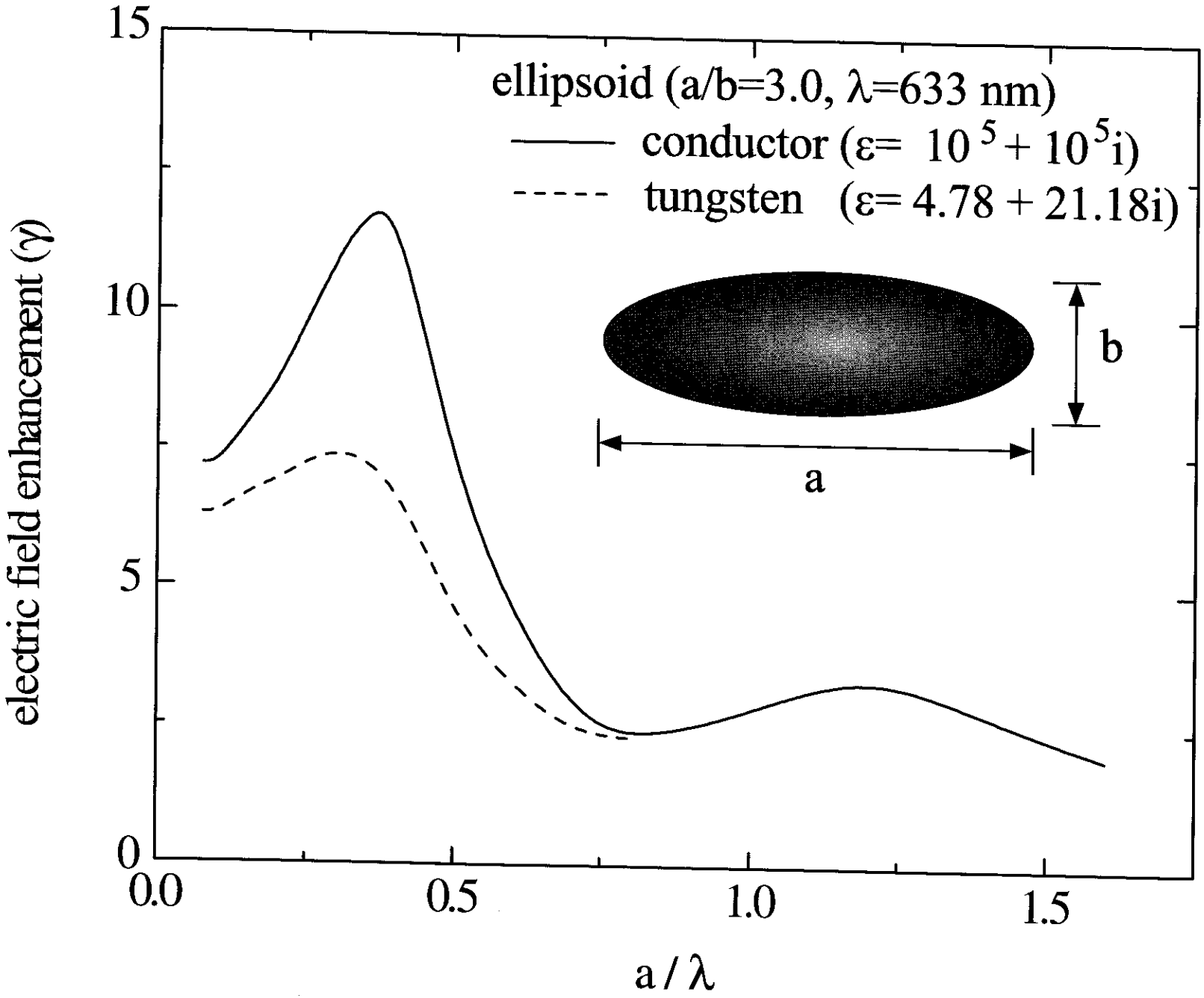

Fig.2 Calculated field enhancement γ at the end of small ellipsoids. The values in the electrostatic limit ($a/\lambda \ll 1$) agrees reasonably well with analytical results. Dephasing effects reduce γ for a greater than 0.5 λ.

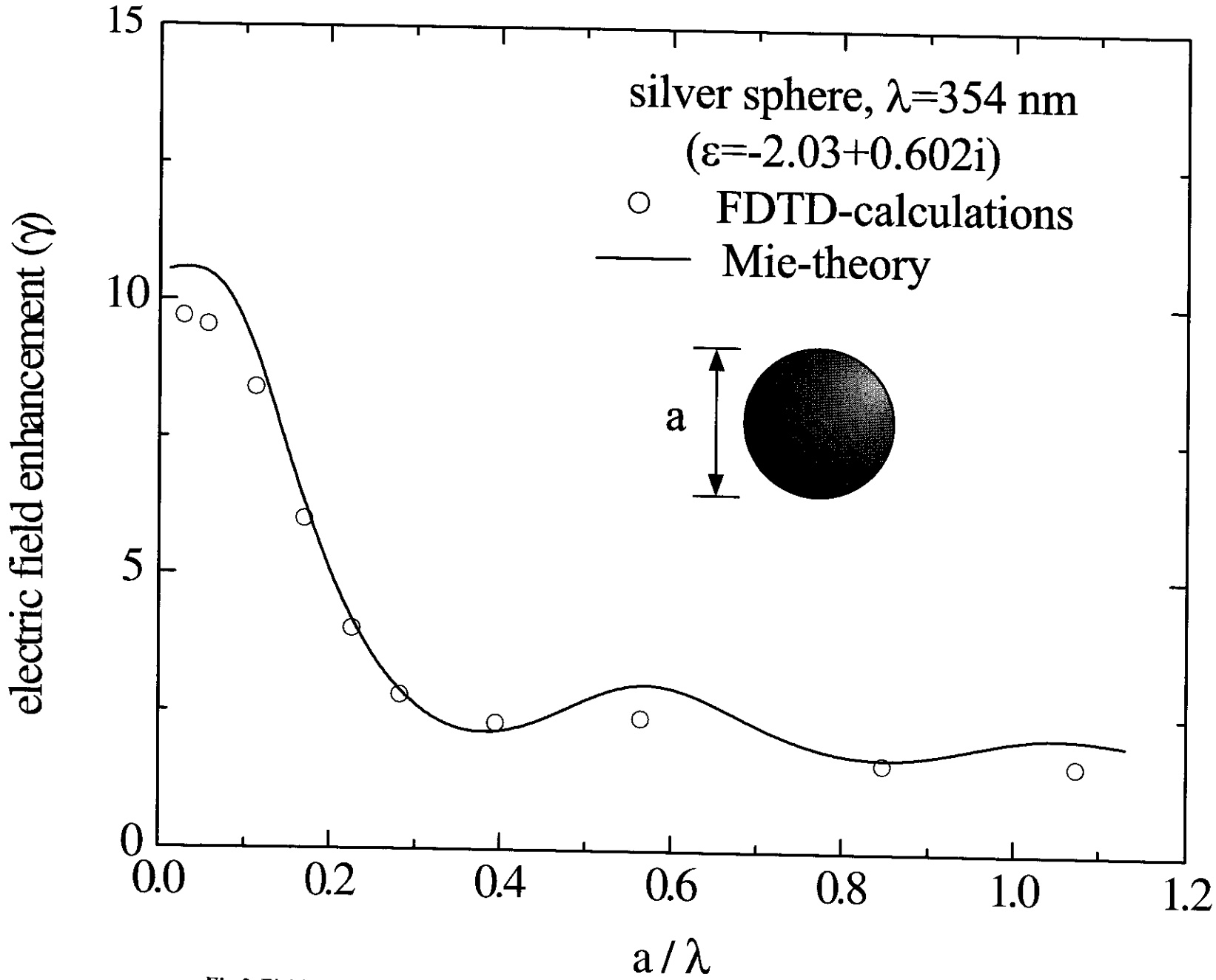

Fig.3 Field enhancement γ for a silver sphere at 354 nm, calculated by MIE and FDTD. Good agreement is found between the two methods. Plasmon resonance dominates when the radius is smaller than $\lambda/10$. Dephasing effects rapidly decrease γ when the size increases.

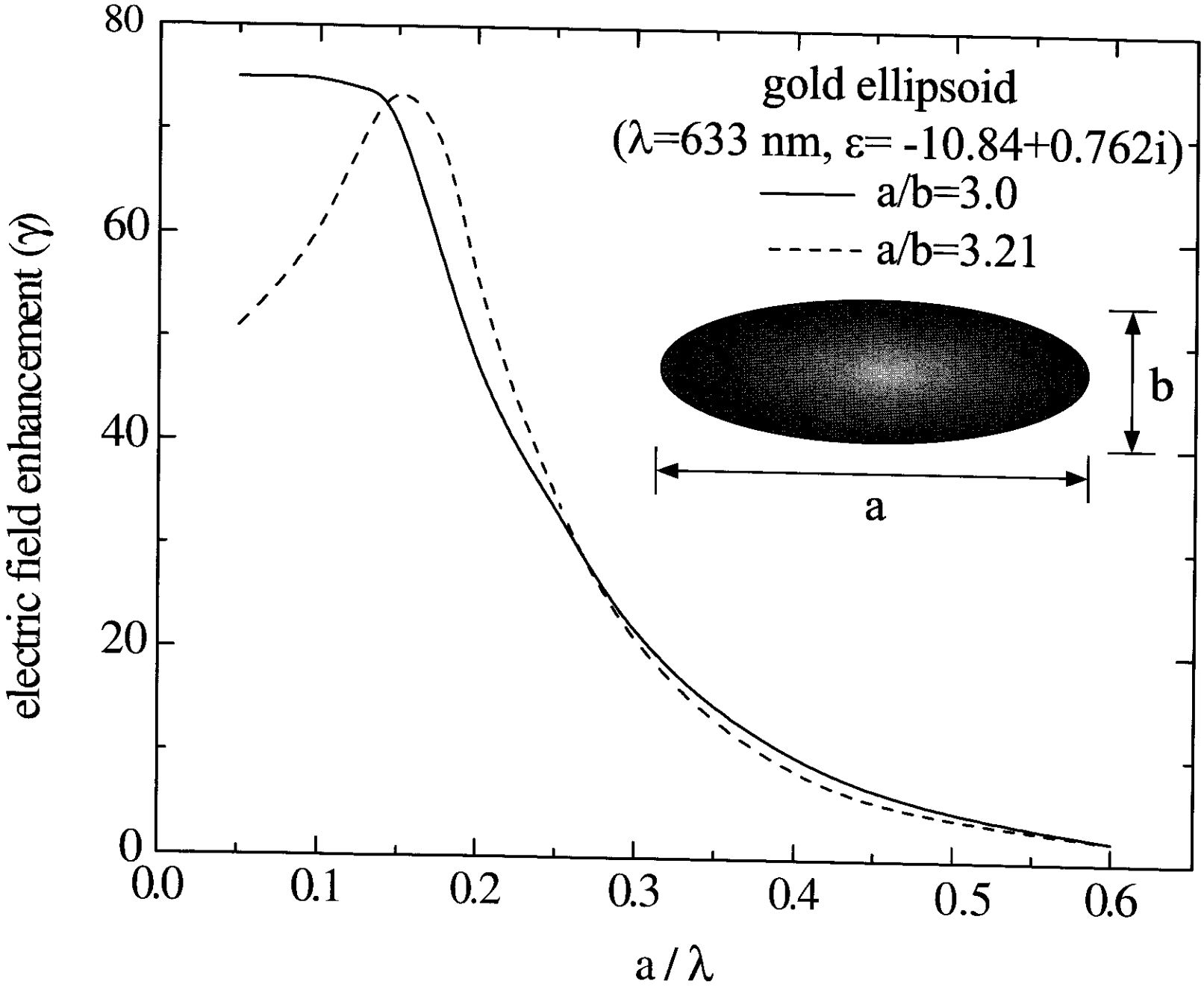

Fig.4 Calculated field enhancement γ for gold ellipsoids at 633 nm. Very large enhancements are found for small size, due to plasmon resonance. Values calculated agree reasonably well with analytical results at small sizes. Dephasing effects drastically decrease γ at larger sizes. When a is greater than 0.5 λ, γ is smaller than 5.

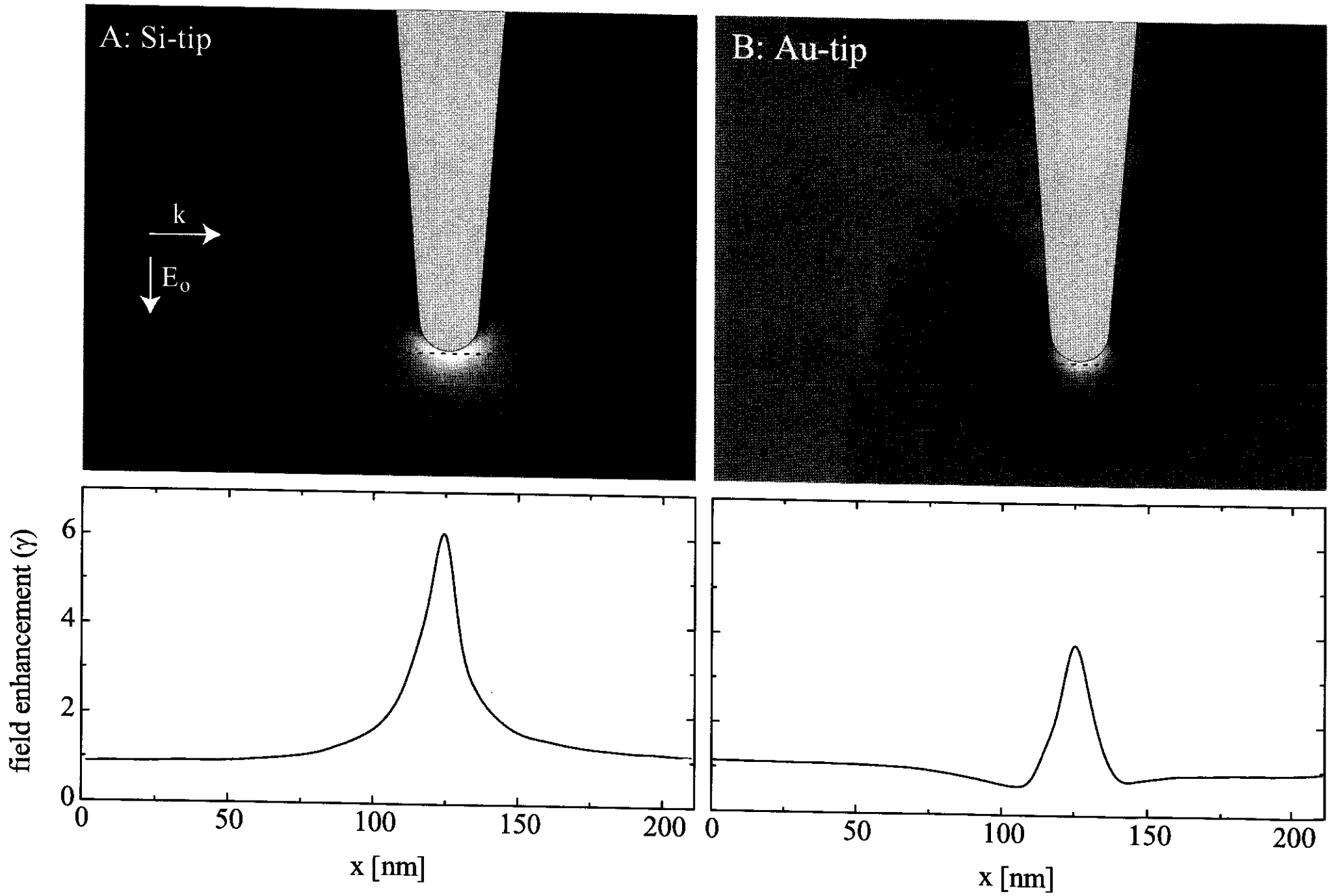

Fig.5 Calculated electric field for silicon and gold tips in a focused beam. Tips are modeled as a narrow cone with a 5 degree angle, terminated by a hemisphere with a 10 nm radius. Focal radius of the incident beam is 0.35 micron. Line plots are given at a distance of 2 nm approximately below the tips.

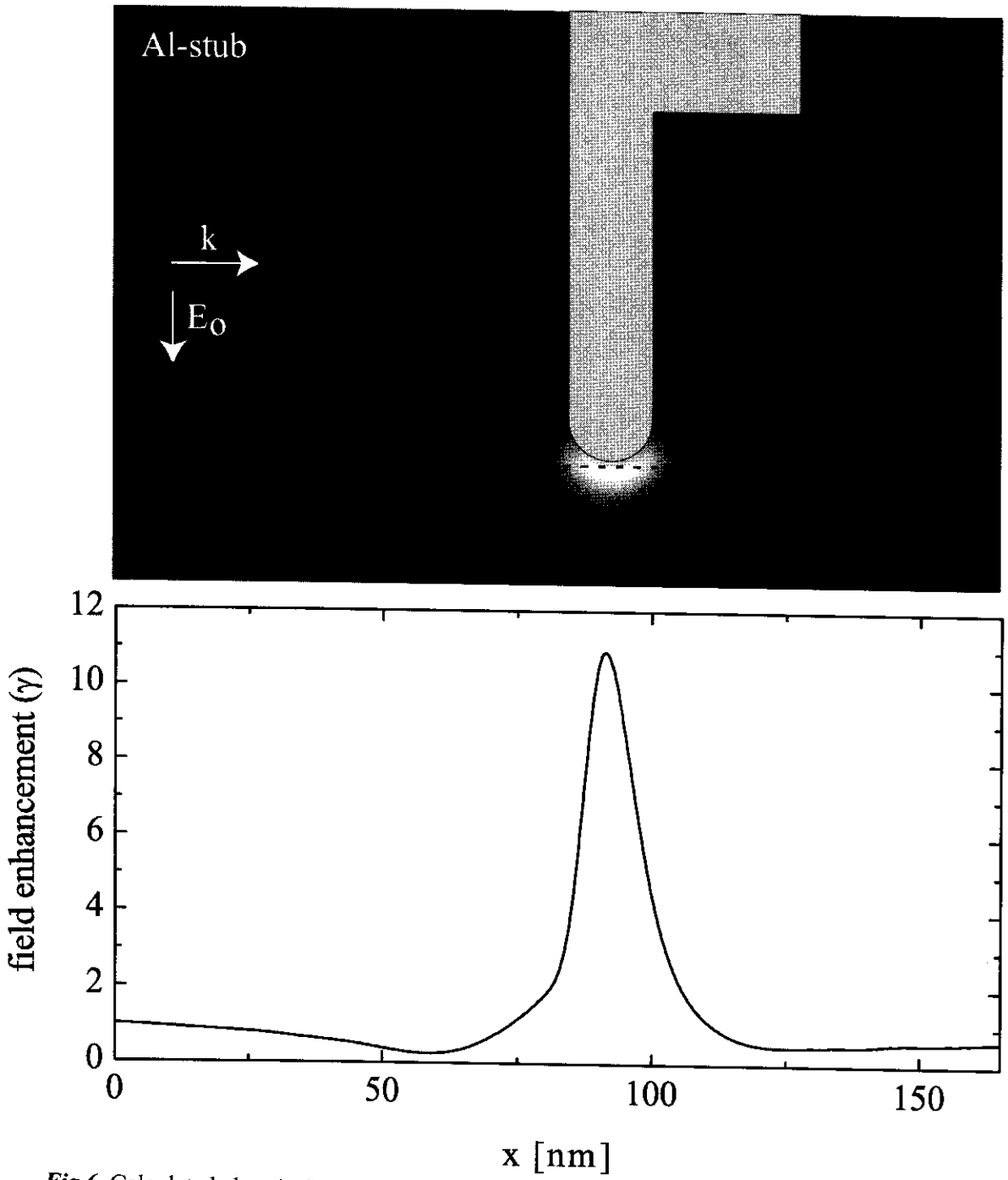

Fig.6 Calculated electric field for an aluminum tip with a discontinuity in a focused beam. Length and diameter of the protrusion are 65nm and 20nm respectively.

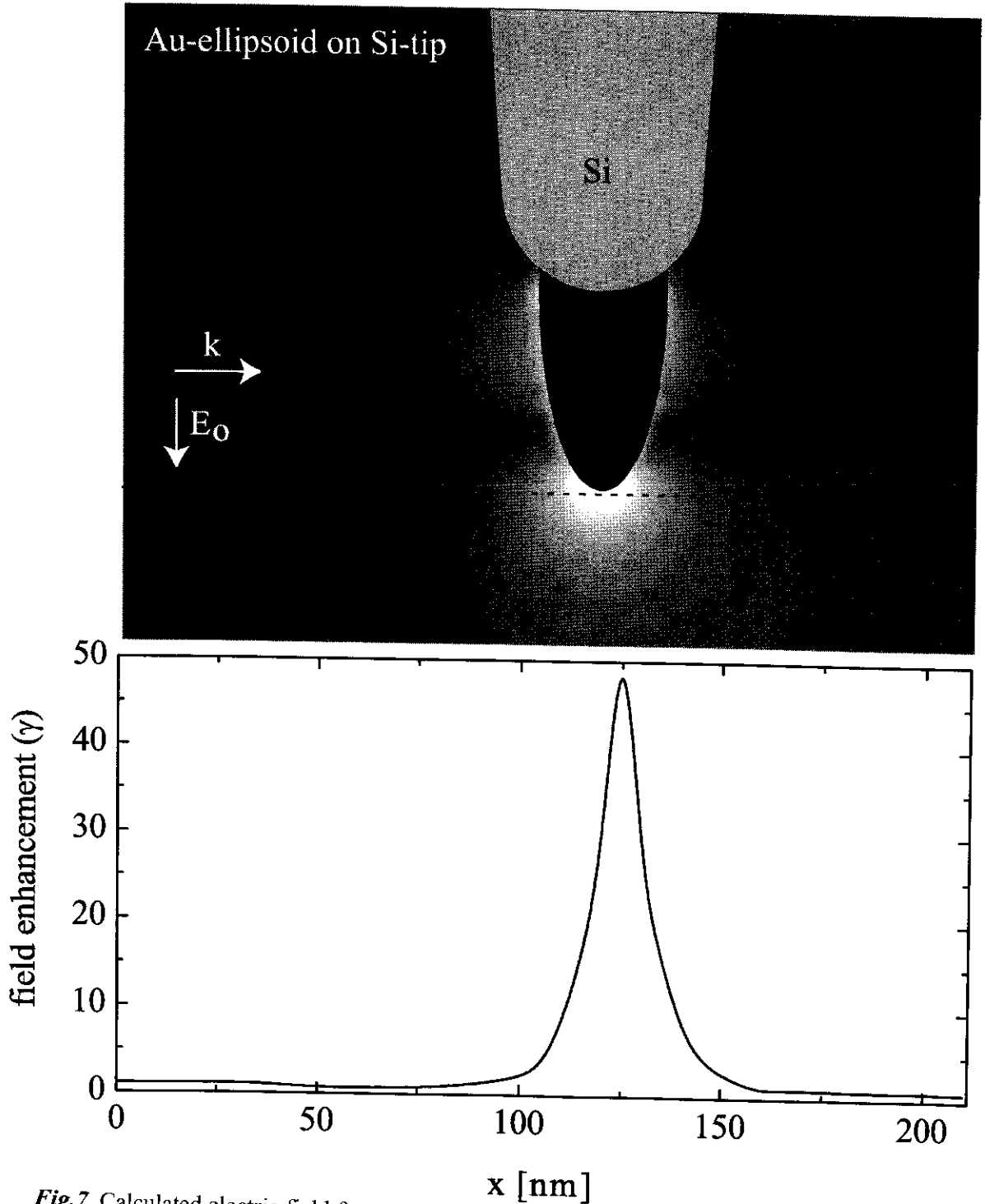

Fig.7 Calculated electric field for a composite tip, a small gold ellipsoid on a wider silicon shank. γ is very large, up to about 50.